The Star Formation Law on sub-kpc Resolution in THINGS

F. Bigiel[1], F. Walter[1], A. Leroy[1], E. Brinks[2], W. J. G. de Blok[3], B. Madore[4], M. D. Thornley[5]

ABSTRACT

We present results from a comprehensive analysis of the relation between HI, H_2, total gas (HI+H_2) and star formation rate surface density ($\Sigma_{\rm HI}$, $\Sigma_{\rm H2}$, $\Sigma_{\rm gas}$ and $\Sigma_{\rm SFR}$ respectively) in 18 nearby galaxies (7 spirals and 11 HI-dominated dwarfs) at 750 pc resolution. We use high resolution HI data from THINGS, CO data from IRAM and BIMA, 24 μm data from the *Spitzer* Space Telescope, and UV data from GALEX. We find that a Schmidt-type power law with index $N = 1.0 \pm 0.2$ relates $\Sigma_{\rm SFR}$ and $\Sigma_{\rm H2}$ across our sample of spiral galaxies, i.e. that H_2 forms stars at a constant efficiency in spirals with an average molecular gas depletion time of $\sim 2 \cdot 10^9$ years. We interpret the linear relation and constant depletion time as evidence that stars are forming in GMCs with approximately uniform properties and that $\Sigma_{\rm H2}$ may be more a measure of the filling fraction of giant molecular clouds than changing conditions in the molecular gas. We find no correlation between $\Sigma_{\rm HI}$ and $\Sigma_{\rm SFR}$. The dwarf galaxies in our sample resemble the outer disks of spirals in $\Sigma_{\rm SFR}$-$\Sigma_{\rm gas}$ space. This is likely due to the similarity of both environments (low–density, low–metallicity, HI–dominated). We furthermore find a sharp saturation of $\Sigma_{\rm HI}$ at $\sim$9 $M_\odot$ pc^{-2} in both the spiral and the dwarf galaxies. For the spirals, we observe gas in excess of this cutoff to be molecular.

Subject headings: radio lines: galaxies — radio lines: ISM — galaxies: ISM — galaxies: evolution

---

[1]Max-Planck-Institut für Astronomie, Königstuhl 17, D-69117, Heidelberg, Germany; bigiel@mpia.de

[2]Centre for Astrophysics Research, University of Hertfordshire, Hatfield AL10 9AB, U.K.

[3]Department of Astronomy, University of Cape Town, Private Bag X3, Rondebosch 7701, South Africa

[4]Observatories of the Carnegie Institution of Washington, Pasadena, CA 91101, USA

[5]Department of Physics and Astronomy, Bucknell University, Lewisburg, PA 17837, USA

1. Introduction

The star formation law, i.e., the relation between gas and star formation (SF) in galaxies, is of great importance for and is widely applied throughout astronomy. Such a relation not only provides valuable constraints on the underlying physics regulating large scale SF in galaxies, it also allows to infer average star formation rates (SFR) from gas measurements and furthermore serves as important input for models of galaxy evolution (e.g. Springel & Hernquist 2003; Boissier & Prantzos 1999; Tan et al. 1999; Krumholz & McKee 2005; Matteucci et al. 2006).

A relation between gas and SF was quantified for the first time from Maarten Schmidt (Schmidt 1959), relating SFR and gas *volume* densities via a power law: $\rho_{\rm SFR} \sim (\rho_{\rm gas})^{\rm n}$. Nowadays, one usually refers to the in other galaxies directly observable *surface* densities when speaking of the star formation law (also referred to as the Schmidt law): $\Sigma_{\rm SFR} \sim (\Sigma_{\rm gas})^{\rm N}$ (e.g. Kennicutt 1989, 1998). For a constant gas scale height, the volume and the surface density description of the SF law are equivalent.

Over the past decades, numerous studies were carried out examining the SF law in various galaxies, using various tracers for the SFRs, studying different physical scales and applying different methodology, e.g., averaging over galactic disks, taking azimuthal averages in tilted rings (radial profiles) or focussing on individual HII regions. Comparing the different results in the literature, one finds $N \approx$ 1-3. In this study, we assess in a sample of 18 nearby galaxies, 7 spirals with H_2 dominated centers and 11 HI dominated dwarfs, whether there are indeed intrinsically different SF laws in different galaxies, or whether there is a common underlying relationship between gas and SF.

2. Data

For our study, we make use of several homogeneous datasets to obtain maps of $\Sigma_{\rm HI}$, $\Sigma_{\rm H2}$, and the SFR surface density, $\Sigma_{\rm SFR}$, in our sample of 18 nearby galaxies.

In order to derive $\Sigma_{\rm HI}$, we use new, high resolution and high sensitivity HI data from THINGS, 'The HI Nearby Galaxy Survey' (Walter et al. 2008). The survey was carried out with the NRAO VLA and provides HI data for a sample of 34 nearby galaxies at distances $2 \leq {\rm D} \leq 15\,{\rm Mpc}$ at $6''$ resolution.

We obtain $\Sigma_{\rm H2}$ from the 'HERA CO-Line Extragalactic Survey' (HERACLES), which was carried out at the IRAM 30m telescope to map the CO $J = 2 \rightarrow 1$ transition in ∼20 nearby galaxies (Leroy et al., in prep.). For one galaxy in our sample we use the CO $J = 1 \rightarrow 0$

map from the 'BIMA Survey of Nearby Galaxies' (BIMA SONG, Helfer et al. 2003). The angular resolution is 11″ and 7″ for the HERACLES and BIMA data, respectively. We combine $\Sigma_{\rm HI}$ and $\Sigma_{\rm H2}$ to derive the neutral gas surface density $\Sigma_{\rm gas}$. Whenever we quote gas surface densities, these values are corrected for inclination.

We combine far UV (FUV) data from the 'GALEX Nearby Galaxy Survey' (NGS, Gil de Paz et al. 2007) and 24 μm data from the '*Spitzer* Infrared Nearby Galaxies Survey' (SINGS, Kennicutt et al. 2003) to derive $\Sigma_{\rm SFR}$. We use the FUV emission to trace SF unobscured by dust and the 24 μm emission to trace SF obscured by dust, i.e., to correct the FUV emission for the effects of extinction (see Leroy et al. 2008).

We construct our sample of 18 galaxies by demanding that each galaxy is part of all datasets: THINGS, the GALEX NGS and SINGS. The 7 spirals must furthermore be part of HERA (or BIMA SONG respectively). We reject galaxies at distances beyond 12 Mpc, to achieve a common spatial resolution of 750 pc, and galaxies with inclinations larger than 70°. For the galaxies in our sample, we carry out a pixel-by-pixel analysis of their optical disks which are defined by the optical radius r_{25}. We therefore extract independent, non-overlapping 750 pc apertures from the optical disk of each galaxy, so that these apertures together cover the entire optical disk.

3. The Spirals

Figure 1 shows the results of the pixel-by-pixel analysis for the 7 spirals in our sample. Shown is $\Sigma_{\rm SFR}$ vs. $\Sigma_{\rm HI}$ (top left), $\Sigma_{\rm SFR}$ vs. $\Sigma_{\rm H2}$ (top right), normalized histograms of $\Sigma_{\rm HI}$ and $\Sigma_{\rm H2}$ (lower left) and $\Sigma_{\rm SFR}$ vs. $\Sigma_{\rm HI+H2} = \Sigma_{\rm gas}$ (lower right). The plots are explained in more detail in the caption.

The $\Sigma_{\rm SFR}$-$\Sigma_{\rm HI}$ distribution in the top left panel shows that the HI saturates at $\Sigma_{\rm HI,sat} \approx 9$ M$_\odot$ pc^{-2}. This is also evident from the HI histogram in the lower left panel. The vertical dashed lines in both panels indicate $\Sigma_{\rm HI,sat}$, which corresponds to the 95th percentile of the HI histogram. Furthermore, one finds from the top left panel that over the range $\Sigma_{\rm HI} = 1.5 - 9$ M$_\odot$ pc^{-2}, which is a typical range of values over the disks of spiral galaxies, several orders of magnitude of $\Sigma_{\rm SFR}$ and star formation efficiency (SFE= $\Sigma_{\rm SFR}/\Sigma_{\rm gas}$) are covered. Thus, $\Sigma_{\rm HI}$ *cannot* be used to predict either $\Sigma_{\rm SFR}$ or the SFE in spiral galaxies.

By contrast, the top right panel shows that $\Sigma_{\rm H2}$ shows no such cutoff. This indicates that where we find gas with surface densities greater than $\Sigma_{\rm HI,sat}$, it is in the molecular phase. As opposed to $\Sigma_{\rm HI}$, $\Sigma_{\rm H2}$ exhibits a clear, monotonic relationship with $\Sigma_{\rm SFR}$ ($\Sigma_{\rm SFR}$-$\Sigma_{\rm H2}$ rank correlation coefficient ∼0.8) down to the sensitivity of our CO data (indicated by the dotted

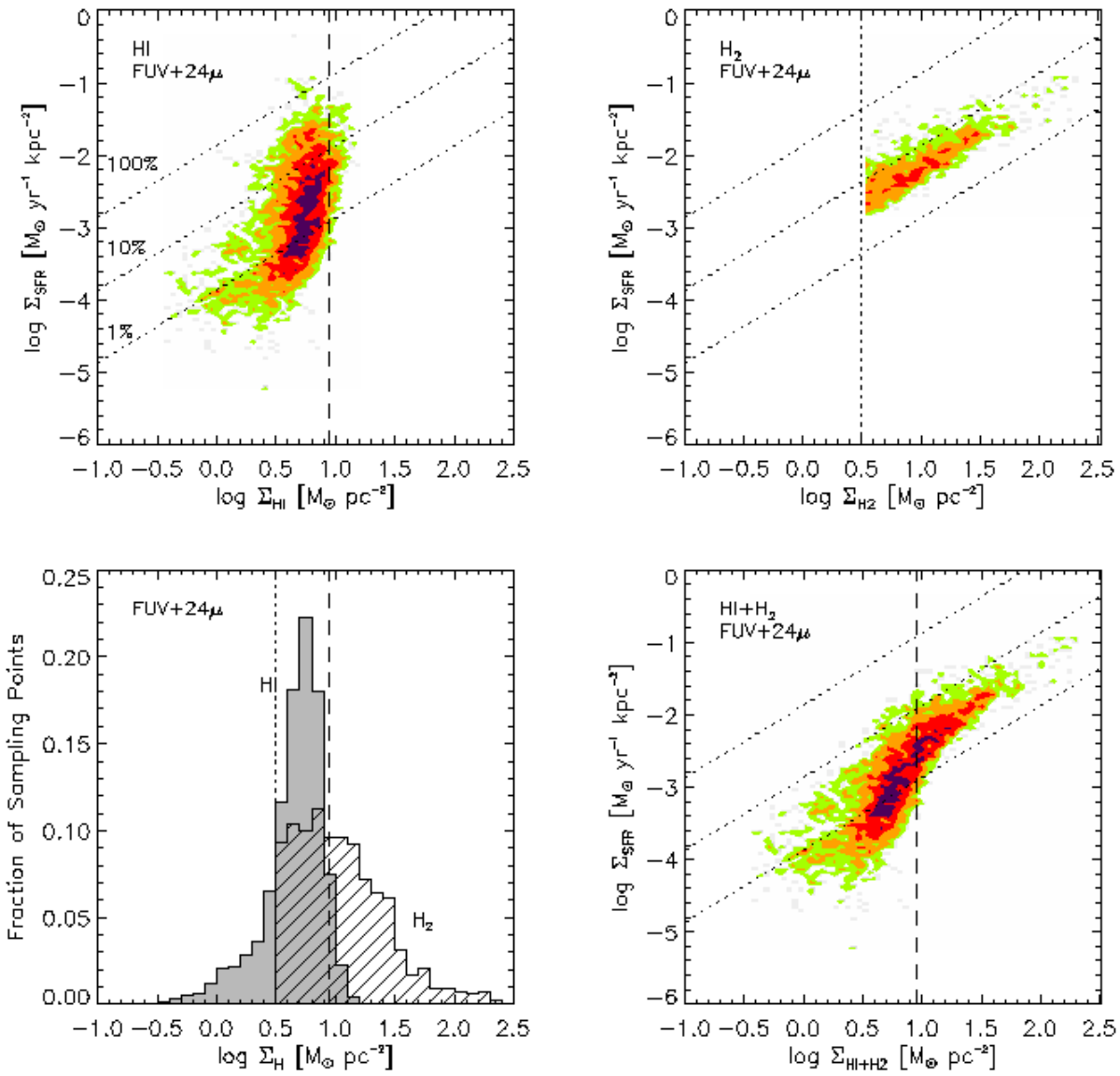

Fig. 1.— Results of the pixel-by-pixel sampling at a resolution of 750 pc for all 7 spiral galaxies plotted together. Top left: $\Sigma_{\rm SFR}$ vs. $\Sigma_{\rm HI}$; top right: $\Sigma_{\rm SFR}$ vs. $\Sigma_{\rm H2}$; middle right: $\Sigma_{\rm SFR}$ vs. $\Sigma_{\rm gas}$. Shown are 2D density plots, i.e., the density of sampling points is color coded. Green, orange, red, and magenta cells show contours of 1, 2, 5, and 10 independent data points per 0.05 dex-wide cell. Diagonal dotted lines show lines of constant star formation efficiency (SFE, defined as $\Sigma_{\rm SFR}/\Sigma_{\rm gas}$) indicating the level of $\Sigma_{\rm SFR}$ needed to consume 1%, 10% and 100% of the gas reservoir (including helium) in 10^8 years. Thus, the lines also correspond to constant gas depletion times of, from top to bottom, 10^8, 10^9, and 10^{10} yrs. Dashed vertical lines in the HI (top left) and total gas (lower right) plots show the surface density where the HI saturates (see text). The dotted vertical line in the top right plot indicates the typical sensitivity for our CO data. The lower left panel shows the normalized distribution of HI and H_2 surface densities in the sample.

vertical line). A power law fit to the data yields a slope of $N = 1.0 \pm 0.2$. Thus, our data suggest a direct proportionality between $\Sigma_{\rm SFR}$ and $\Sigma_{\rm H2}$. We derive a mean H_2 gas depletion time of $1.8 \cdot 10^9$ yrs, with an RMS scatter of $0.7 \cdot 10^9$ yrs.

For the $\Sigma_{\rm SFR}$-$\Sigma_{\rm gas}$ distribution in the lower right panel, one finds a clear 'knee' at the transition from an HI to an H_2 dominated ISM. In general, $\Sigma_{\rm gas}$ is thus also not well suited to predict $\Sigma_{\rm SFR}$ or the SFE.

Our power law slope of N=1.0±0.2 is shallower than the slope of N≈1.4 derived by Kennicutt (1998), whose fit is largely driven by starburst galaxies, and similar power law slopes derived for starbust galaxies at low and high redshift (e.g. Gao & Solomon 2004; Riechers et al. 2007).

Most of the mass in Galactic GMCs is in clouds with $M_{\rm H2} \approx 5 \cdot 10^5 - 10^6$ $M_\odot$ (e.g. Blitz 1993). For our 750 pc resolution elements, and our sensitivity of $\Sigma_{\rm H2} = 3$ $M_\odot$ pc^{-2}, we can detect a minimum mass along a line of sight of $\sim 1.5 \cdot 10^6$ $M_\odot$. Thus, a significant H_2 detection corresponds to at least a few GMCs in our beam. But because we probe only normal star forming spirals (i.e. starburst galaxies are not part of our sample), and because we use area-weighted (i.e. pixel-by-pixel) sampling, our distributions are dominated by moderate gas surface densities up to $\sim$50 $M_\odot$ pc^{-2}. The typical surface density of a Galactic GMC is $\sim 170\,M_\odot$ pc^{-2} (Solomon et al. 1987). Our measured surface densities are thus consistent with Galactic GMCs filling less than 1/3 of our beam on average. We therefore interpret our measurement of $N = 1.0 \pm 0.2$ as suggestive of more or less universal GMC properties in nearby spiral galaxies, i.e., $\Sigma_{\rm H2}$ most likely just represents the beam filling fraction of GMCs.

Summarized, our results indicate that GMC properties, in particular their SFEs, are relatively universal across our sample of normal star forming spirals and that the Schmidt law apparently consists of distinctly different physical regimes.

4. The Dwarfs

For the HI dominated dwarf galaxies we neglect the contribution of molecular gas (H_2) to the total neutral gas budget. For most of these galaxies, the CO content is either measured or constrained by a significant upper limit and in each case, the ISM is well-established to be HI dominated.

Figure 2 compares the pixel-by-pixel distribution for the dwarf galaxies (colored contours) to the distribution for the spirals. Every panel compares the spiral distribution for a different regime in galactocentric radius (black contours) to the dwarf distribution.

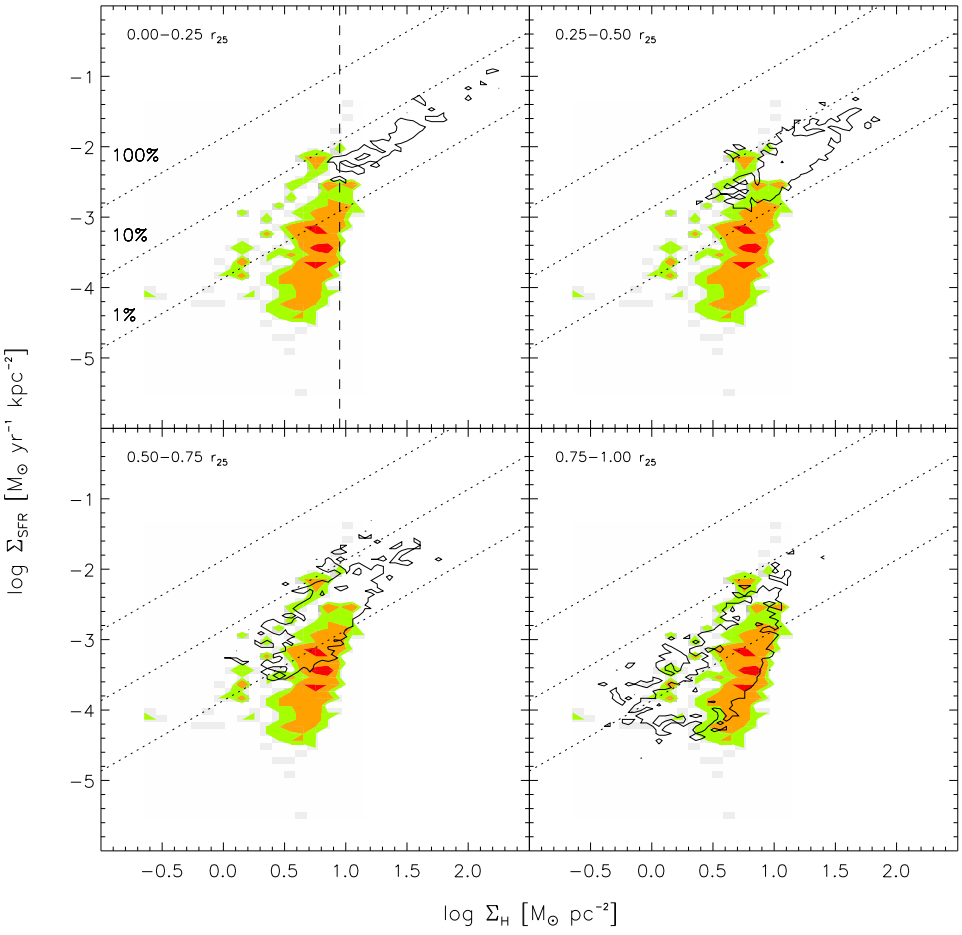

Fig. 2.— Results of the pixel-by-pixel sampling at a resolution of 750 pc for the 11 HI dominated dwarf galaxies in our sample (colored contours). All four panels show the same $\Sigma_{\rm SFR}$-$\Sigma_{\rm HI}$ distribution. Green, yellow, and red contours show 1, 2, and 5 sampling points per cell. The diagonal dotted lines and all other plot parameters are the same as in Figure 1. Plotted on top of the dwarf distribution is the lowest contour (green) from the total gas distribution of the spirals (see bottom right panel of Figure 1), but for different ranges in galactocentric radius in each panel. Thus, each panel compares the distribution of the HI dominated galaxies to that in spiral galaxies from a particular radial range (given in the top left corner of each panel) . The best agreement is seen in the bottom right panel, in which the black contour shows sampling data from 0.75–1.0 r_{25} in spiral galaxies.

One finds that the $\Sigma_{\rm SFR}$-$\Sigma_{\rm gas}$ distribution for the dwarf galaxies overlaps the distribution for the outer disks of the spirals (bottom right panel in Figure 2). Both regimes, i.e. the optical disks in dwarfs and the outer disks in spirals, have many conditions in common: high atomic-to-molecular gas ratio, low metallicities, low dust-to-gas ratio and relatively weak stellar potential wells. These common environmental factors may lead to similar relationships between $\Sigma_{\rm SFR}$ and $\Sigma_{\rm gas}$ in both regimes.

Furthermore, the dwarfs show the same saturation in $\Sigma_{\rm HI}$ like the spirals (indicated by the vertical dashed line). This seems somewhat counter-intuitive, as, due to comparatively low metallicities (and thus lower dust content), shallow potential wells, lower gas densities, and more intense radiation fields, one might expect conditions in the ISM of many of these galaxies to be less favorable to the formation of H_2 from HI and therefore large reservoirs of HI to survive in these galaxies at columns where the ISM is mostly molecular in a spiral.

We thank the local and scientific organizing committees for an illuminating conference. THINGS is based on VLA data; The VLA is operated by the National Radio Astronomy Observatory, which is a facility of the National Science Foundation operated under cooperative agreement by Associated Universities, Inc. HERACLES uses the IRAM 30m; IRAM is supported by CNRS/INSU (France), the MPG (Germany) and the IGN (Spain). This work is furthermore based on observations made with the *Spitzer Space Telescope*, which is operated by the Jet Propulsion Laboratory (JPL), California Institute of Technology under NASA contract 1407. Support for this work was provided by NASA and through JPL Contract 125509. We thank the SINGS, GALEX NGS, and BIMA SONG teams for making their high quality data publicly available.

REFERENCES

Blitz, L. 1993, Protostars and Planets III, 125

Boissier, S. & Prantzos, N. 1999, MNRAS, 307, 857

Gao, Y. & Solomon, P. M. 2004, ApJ, 606, 271

Gil de Paz, A., et al. 2007, ApJS, 173, 185

Helfer, T. T., Thornley, M. D., Regan, M. W., Wong, T., Sheth, K., Vogel, S. N., Blitz, L. & Bock, D. C.-J. 2003, ApJS, 145, 259

Kennicutt, R. C. 1989, ApJ, 344, 685

Kennicutt, R. C. 1998, ApJ, 498, 541

Kennicutt, R. C., Jr., et al. 2003, PASP, 115, 928

Krumholz, M. R. & McKee, C. F. 2005, ApJ, 630, 250

Leroy, A., et al. 2008, AJ, submitted

Madore, B. F. 1977, MNRAS, 178, 1

Matteucci, F., Panagia, N., Pipino, A., Mannucci, F., Recchi, S. & Della Valle, M. 2006, MNRAS, 372, 265

Riechers, D. A., Walter, F., Carilli, C. L. & Bertoldi, F. 2007, ApJ, 671, L13

Schmidt, M. 1959, ApJ, 129, 243

Solomon, P. M., Rivolo, A. R., Barrett, J. & Yahil, A. 1987, ApJ, 319, 730

Springel, V. & Hernquist, L. 2003, MNRAS, 339, 289

Tan, J. C., Silk, J. & Balland, C. 1999, ApJ, 522, 579

Walter, F. 2008, AJ, submitted